



## Textile Dyes removal from industrial waste water by mytilus edulis shells

I. Maghri<sup>1</sup>, A. Kenz<sup>1</sup>, M. Elkouali<sup>1</sup>, O. Tanane<sup>1\*</sup>, M. Talbi<sup>1</sup>

<sup>1</sup>Laboratory of analytical chemistry and physico-chemistry of materials, faculty of sciences Ben M'Sik B.P. 7955, 20702, Casablanca, Morocco.

Received in 28 Sept 2011, Revised 19 Oct 2011, Accepted 19 Oct 2011.

\*Corresponding author: Email: [o.tanane@gmail.com](mailto:o.tanane@gmail.com), Tel: +212 664 226 815

### Abstract

Effluent from the textile industry is loaded of non-biodegradable dyes which make them difficult to apply biological treatments. Several techniques have been employed to remove dyes from wastewater; biosorption is being the most used actually. The marine biomaterial *Mytilus Edulis* shells were used as a new low-cost biological sorbent for the removal of textile dyes (Indigo Carmine and Methylene Blue) from aqueous solutions. The *Mytilus Edulis* shells were characterized by several techniques XRD, XRF, FTIR and SEM. A sample of *Mytilus Edulis* shells has been utilized as a sorbent for uptake Indigo Carmine and Methylene Blue. Experiments were conducted to investigate the biosorption characteristics of dyes by *Mytilus Edulis* shells. Operating variables studied were contact time, shells quantity, granulometry, initial dye concentration, temperature and pH. Biosorption capacity seems to be enhanced by increasing the biosorbent mass. Rising the temperature has also a positive effect on dye removal rate. Initial pH played the most important effect on the adsorbed amount of dyes. Pre-treating shells increased considerably the biosorption capacity. The constants in the Freundlich, Langmuir isotherms, the pseudo-first and pseudo-second orders kinetics models were calculated. Besides, the sorption study has showed that the *Mytilus Edulis* sorption was good and favourable. The shells biosorption capacity was compared to biosorption capacity of wood sawdust, marine algae and activated carbon. *Mytilus Edulis* shell is an effective sorbent to treat dye wastewater.

**Keywords:** Dye wastewater, Indigo Carmine, Methylene Blue, Biosorption, *Mytilus Edulis* shells.

### 1.Introduction

The mussel is one of very abundant marine bivalve mollusc and occupies varied ecological niches in the whole world; one finds it in the majority of polar and moderated water. In the area of the Gulf, the mussel lives on the rocky shores, along the coasts, of bays and with the mouth of the rivers, where they are fixed at immersed surfaces. The mussel has a shell playing a role of exosquelette from 6 to 8 cm length. It keeps its shell throughout its life. The structure very porous of the *Mytilus Edulis* shells aroused our interest, these mussels are nourished by filtration (it filters 10 times more water than oysters) [1-2] and they present a model of biosorption interesting to study.

The world annual production of dyes is estimated at more than 80000 tons used mainly in food industries, cosmetics, paper mills and especially in textile industries which absorb alone more than 70% of the produced total quantity [3]. The intense use of the synthetic dyes in these various industries generates sources of considerable pollution of the environment. Indeed, 10 to 15% of the quantity of dyes used is rejected into the natural environment [4]. These dyes, in addition to dangerous pollution that they can generate, constitute because of their toxicity a potential danger to both Man and environment [5].

The Indigo Carmine is classified as strongly toxic dyes [6], its contact with the human body can cause irritations of skin and eye. It can also cause permanent damage with the cornea and the conjunctive one. It was also reported that it has effects of hypertension, cardiovascular and respiratory. It can also cause gastro-intestinal irritation with nausea, vomiting and diarrhoea. The tests of toxicity of this dye indicated long-term

toxicity at the mice and the short-term toxicity in the pig. Moreover, Indigo Carmine causes an immediate reduction of the mobility of sperms to man after direct exposure [7].

In the same case, Methylene Blue, which has a recognized toxicity, is regarded as a very dangerous pollutant on the environment even when there exists in small quantities.

## 2. Experimental

### 2.1. Shells preparation

The "Mytilus Edulis" shells were collected from the zone "Sidi Abd Rahman" in the littoral of Casablanca (Morocco). After collection, the shells were washed with distilled water to eliminate the sands and the undesirable remains stuck to shells external surface. They were dried thereafter in free air. After drying, the shells were crushed in a mortar which was then filtered in a series of standardized sieves AFNOR.

The mineralogical composition of the Mytilus Edulis shells were deduced by X-Ray diffraction (XRD) and Spectroscopy of X-Ray fluorescence (XRF), the study on a molecular scale is obtained by Infra-red Spectroscopy (FTIR).

### 2.2. Characterization methods

#### 2.2.1. X-Ray powder diffraction (XRD)

X-ray diffraction patterns were obtained with a Philips X'Pert PRO powder diffractometer using copper anticathode  $\lambda(\text{Cu}) = 1.5418\text{\AA}$  in the area of  $2\theta = 10^\circ$  with  $2\theta = 60^\circ$ .

#### 2.2.2. Spectroscopy of x-ray fluorescence (XRF)

The chemical analysis of the Mytilus Edulis shells was carried out using a spectrometer of *x-ray fluorescence* with dispersion wavelength using sequential spectrometer with a measurement channel based on a single goniometer covering the full range of measurement (Be to U). The sample is prepared in the form of pastille and then carried at the temperature of  $1000^\circ\text{C}$  in an induction furnace.

#### 2.2.3. Spectrophotometry Infra-red (FTIR) and scanning electron microscope (SEM)

The infra-red spectra of the samples were recorded between  $400$  and  $4000\text{ cm}^{-1}$  with a VERTEX 70 spectrophotometer. The pastille was obtained by crushing  $1\text{ mg}$  of sample in  $99\text{ mg}$  of KBr then dried at  $100^\circ\text{C}$  during 2 hours, while Scanning electron microscope is a technique of electron microscopy based on the principle of electron-matter interactions, capable of producing high-resolution images of the surface of a sample. The scanning principle is to explore the surface of the sample by successive lines and transmit the sensor signal to a CRT with scavenging exactly synchronized with the incident beam. This analysis technique can get an idea on the Morphology of shells.

### 2.3. Biosorption studies

Biosorption of Indigo Carmine and Methylene blue was carried out in a batch process by varying Mytilus Edulis shell dose, biosorptive concentration, pH of medium and temperature. A weighed sample of Mytilus Edulis shell was mixed with  $75\text{ ml}$  Indigo Carmine solution of known concentration. The mixture, in a  $100\text{ml}$  conical flask, was shaken in the water bath of thermostat at particular temperature for 3h. In all cases, biosorption equilibrium was reached within 60 mn. The mixture was allowed to settle and was centrifuged. The Indigo concentration in the supernatant was determined with an UV-Vis spectrophotometer (UV mini 1240).

### 2.4. Biosorption isotherms

The Biosorption data from experiments were fitted with:

#### 2.4.1. Freundlich Isotherm: [8]

$$q_e = K_f \cdot C_e \quad (1)$$

Where,  $K_f$  and  $n$  are constants indicating biosorption capacity and biosorption intensity, respectively. The constants were obtained from the plots of the linearized equations:

$$\log q_e = \log K_f + n \log C_e \quad (2)$$

Another use of the results is to plot the variation of the distribution coefficient  $K_d$  as a function of  $q_e$  in logarithmic scale:

$$\log K_d = \left( \frac{1}{n} \right) \log K_F + \frac{[(n-1)]}{n} (\log q_e) \quad (3)$$

#### 2.4.2. Langmuir Isotherm:

$$\frac{q_e}{q_m} = \theta = \frac{K_L \cdot C_e}{(1 + K_L \cdot C_e)} \quad (4)$$

Where,  $C_e$  is the dye residual concentration in solution (mg/l);  $q_{\max}$  the maximum specific uptake corresponding to sites saturation (mg.g<sup>-1</sup>) and  $K_L$  the biomass-dye binding affinity (l.mg<sup>-1</sup>), development of this equation lead to linear forms of Langmuir isotherm. Among, the five forms are presented in the table 1 [9].

**Table 1:** The Five forms of Langmuir isotherm

Langmuir 1	$\frac{1}{q_e} = \frac{1}{C_e} \frac{1}{K_L \cdot q_m} + \frac{1}{q_m}$
Langmuir 2	$\frac{C_e}{q_e} = C_e \frac{1}{q_m} + \frac{1}{q_m \cdot K_L}$
Langmuir 3	$q_e = - \frac{1}{K_L} \frac{q_e}{C_e} + q_m$
Langmuir 4	$\frac{q_e}{C_e} = - K_L \cdot q_e + K_L \cdot q_m$
Langmuir 5	$\frac{1}{C_e} = K_L \cdot q_m \frac{1}{q_e} - K_L$

#### 2.4.3. Elovich Isotherm:

Elovich model [10] is based on an expansion kinetics assuming that the adsorption sites increases exponentially with the adsorption, which implies a multi-layer adsorption. When it is used, it is expressed by the equation (5) [11]:

$$\frac{q_e}{q_m} = \theta = K_E \cdot C_e \cdot \exp \left( - \frac{q_e}{q_m} \right) \quad (5)$$

$K_E$  is the Elovich constante (L.mg<sup>-1</sup>), the linearization of Elovich model conduct to:

$$\ln \frac{q_e}{C_e} = - \left( \frac{q_e}{q_m} \right) + \ln (K_E \cdot q_m) \quad (6)$$

### 2.4.3. Temkin Isotherm:

The Temkin model [12] assumes that when the gas absorption, heat of adsorption due to interactions with the adsorbate decreases linearly with the recovery rate  $q$ . It is an application of the Gibbs adsorption where the surface is considered energetically homogeneous [13]. Several authors [10, 14-18] propose to use this model in the liquid phase, tracing  $q_e$  based  $\ln C_e$ :

$$\frac{q_e}{q_{max}} = \theta = \left( \frac{RT}{\Delta Q} \right) \ln (K_T \cdot C_e) \quad (7)$$

Where  $R = 8.314 \text{ J.mol}^{-1}.\text{K}^{-1}$ ,  $T$ , absolute temperature (K),  $\Delta Q$ , energy change of adsorption ( $\text{J.mol}^{-1}$ ),  $K_T$ , Temkin constant ( $\text{L.mg}^{-1}$ ).

### 2.5. Biosorption kinetics

Biosorption parameters were computed with:

#### 2.5.1. Pseudo first order model:

The model of the first order is generally expressed by [19]:

$$\frac{dq_t}{dt} = K_{1app} \cdot (q_e - q_t) \quad (8)$$

Which carry out, after integration, to [20]:

$$\ln (q_e - q_t) = \ln (q_e) - K_{1app} \cdot t \quad (9)$$

#### 2.5.2. Pseudo second order model:

It is an equation which is often employed on the representation of kinetics of biosorption. It is presented in the form [21]:

$$\frac{dq_t}{dt} = K_{2app} (q_e - q_t)^2 \quad (10)$$

The integration of the equation (10) permits to obtaining the equation (11) [22]:

$$\left( \frac{1}{q_t} \right) = \left( \frac{1}{K_{2app} \cdot q_e^2} \right) \cdot \frac{1}{t} + \left( \frac{1}{q_e} \right) \quad (11)$$

This presents the linearization of the second-class equation; it is the equation which helps us to extract the parameters of the second order.

## 3. Results and discussions

### 3.1. Shell Characterization

#### 3.1.1. X-ray powder diffraction (XRPD)

The figure 1 displays the XRD diffraction patterns of *Mytilus Edulis* shells which showed that shells are made of Aragonite " $\text{MgCO}_3$ " with very intense characteristic lines and Calcite " $\text{CaCO}_3$ " with characteristic lines relatively weak compared to Aragonite. The shell "*Mytilus Edulis*" consists of an intimate and complex assembly of calcium carbonate (called limestone). Calcium can be partially replaced by other elements such as Mg.

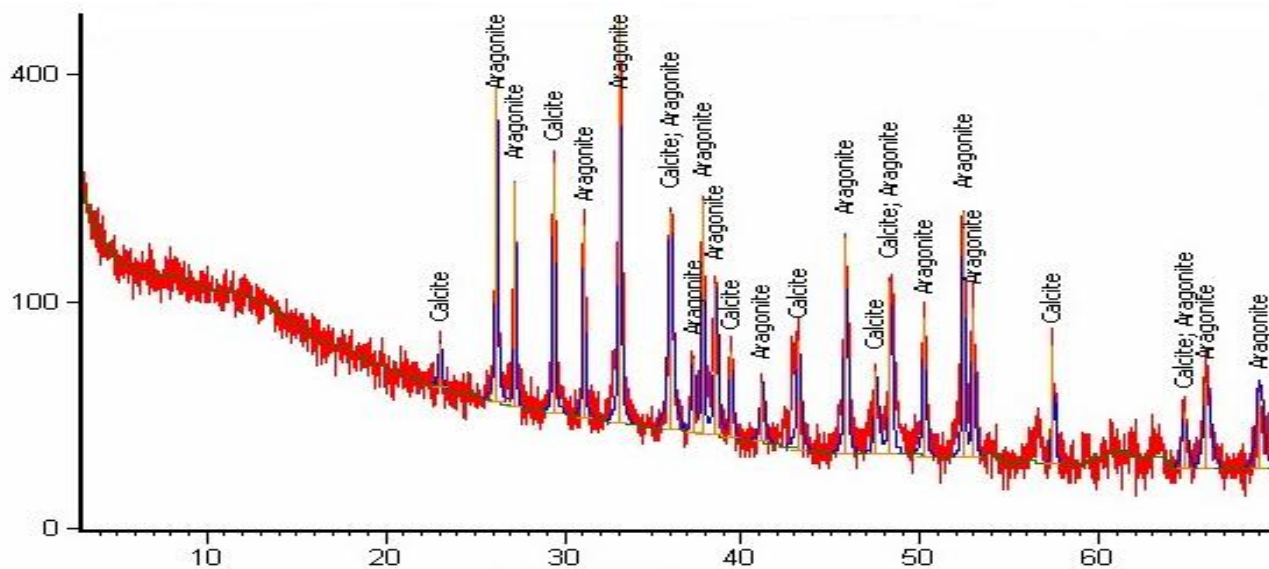


**Figure 1:** XRD spectrum of Mytilus Edulis shells

### 3.1.2. X-Ray Fluorescence Spectroscopy (XRF)

The table 2 shows the experimental data of Mytilus Edulis shells composition. The principal components of shells are CaO, CuO and SiO<sub>2</sub> with 48.93%; 1.32% and 1.06 % respectively. The CaO present in significant quantity confirms the presence of carbonates. The contents of the other elements (Na<sub>2</sub>O, ZnO, MgO, Fe<sub>2</sub>O<sub>3</sub> and P<sub>2</sub>O<sub>5</sub>) are rather weak. The loss of fire is very high (46%), it can be explained by the presence of certain organics elements not detected.

### 3.1.3. Spectrophotometry Infra-red (FTIR)

The FT-IR spectra of Mytilus Edulis shells are shown in figure 2 in the range 400–3700 cm<sup>-1</sup>. The IR spectrum shows band at 1473.7cm<sup>-1</sup>, which are assigned to vibrations of C-O [23]. The band at about 1000 et 1100 cm<sup>-1</sup> exactly at 1082.7cm<sup>-1</sup> is due to internal vibrations of Si-O [24-25], whereas the bands at 860.9 cm<sup>-1</sup> is due to vibrations related to vibrations of calcite [26]. The bands at about 742.6 et 699.9 cm<sup>-1</sup>, assigned respectively to vibrations of quartz [27].

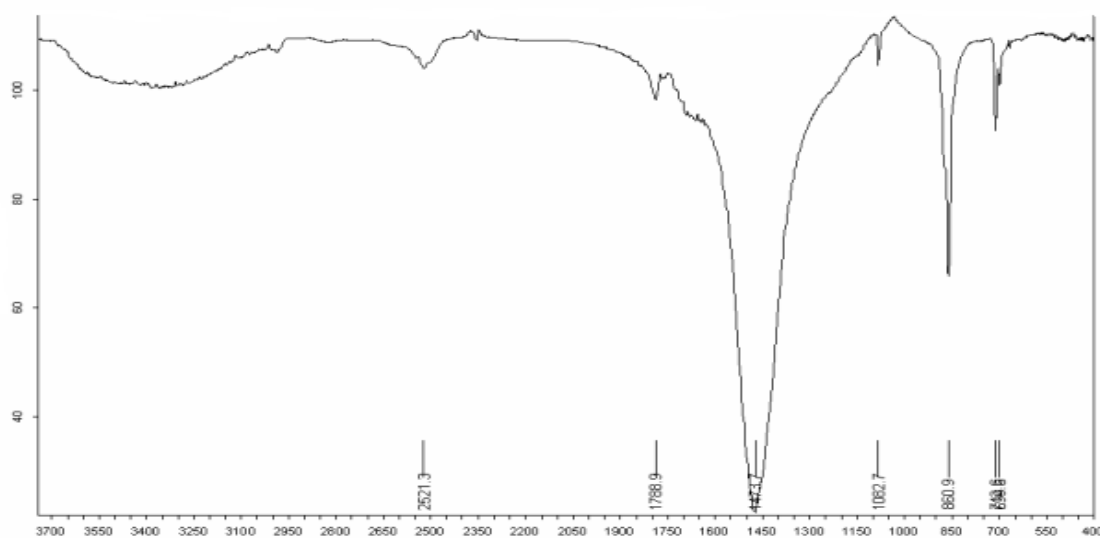


**Figure 2:** FT-IR spectra of Mytilus Edulis shells in the frequency region (400–3700 cm<sup>-1</sup>).

### 3.1.4. Scanning microscopy Electronics (SEM)

The figure 3 below shows a view from external side of a shell, the shells have a very porous structure. This structure makes the shells as good biosorption support, the pores acts as a container for the dye molecules.

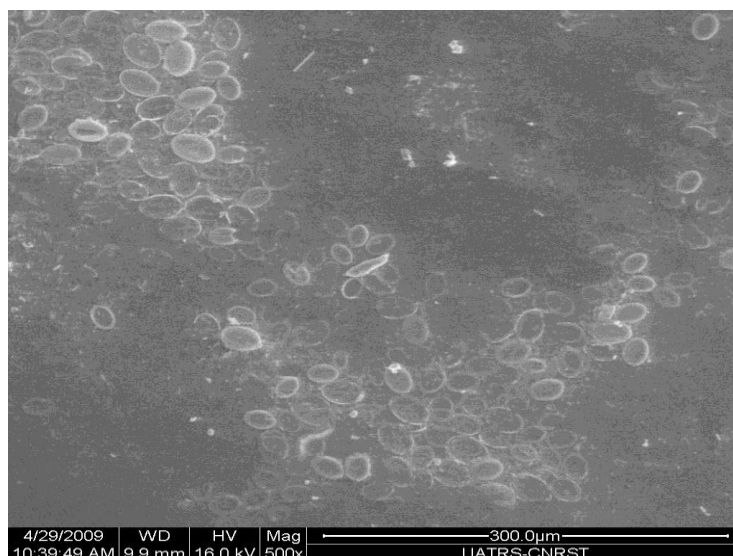


**Figure 3:** View of external side of Mytilus Edulis shell

### 3.2. Biosorption study

The effects of various experimental parameters have been investigated using a batch biosorption technique to obtain information on treating effluents from the dye industry.

#### 3.2.1. pH effect on biosorption of dyes

When the pH is between 3 and 10, there is no precipitation of Methylene Blue and when the pH is between 2 and 3 (less than 3), there is no precipitation of Indigo Carmine (figure 4), this is why we carried out all tests in this interval biosorption

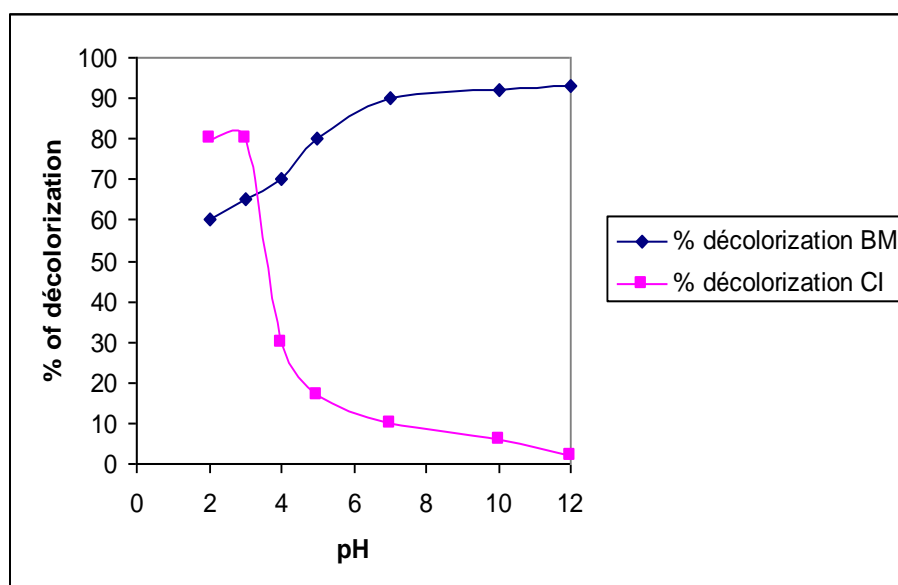
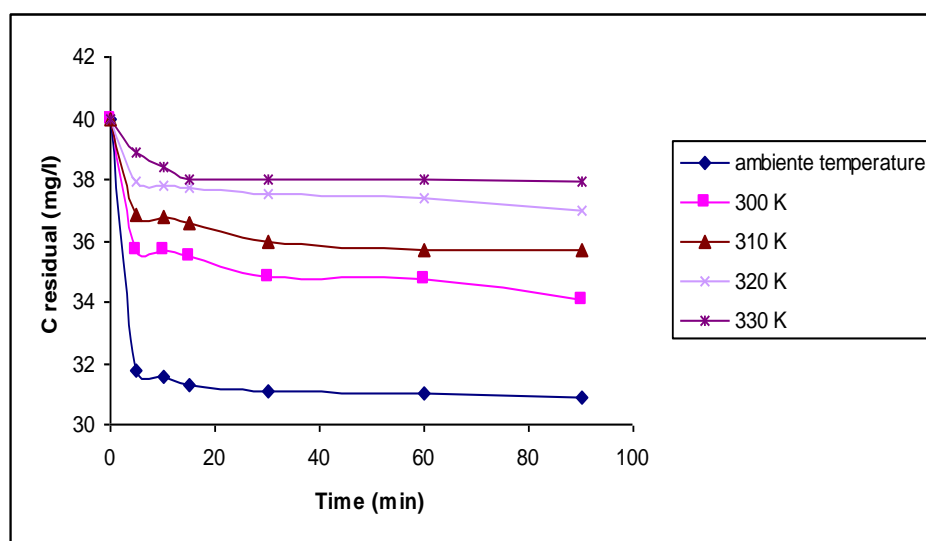


**Figure 4:** Variation of decolorization percentage with pH

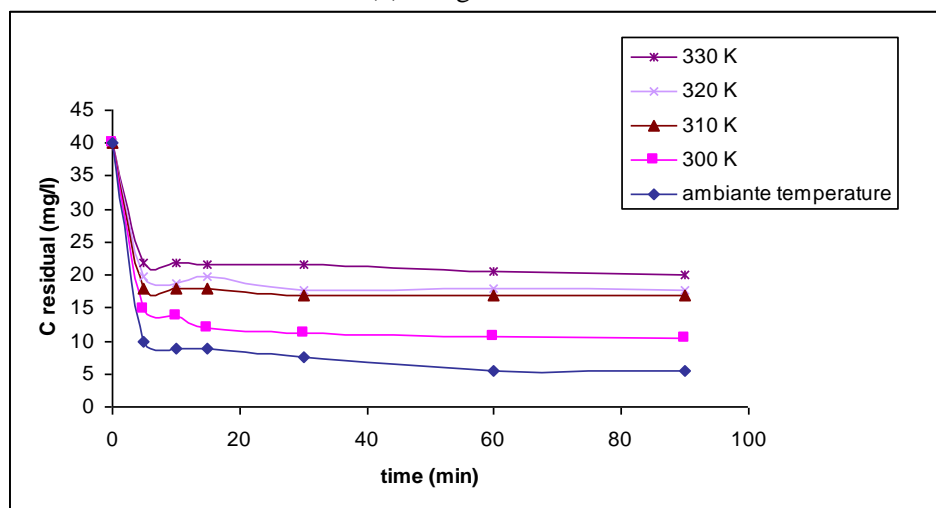
The figure 4 indicates that the percentage % of decolorization is higher in acid phase and decreases with increasing initial pH. This result may be due to the influence of solution pH on both the surface of the shells and the ionization state of ionisable organic molecules of this dye. While the Methylene Blue percentage of decolorization is low in acid phase, it increases with decreasing initial pH

### 3.2.2. Mixture temperature effect study

Various textile dye effluents are produced at relatively high temperature; therefore, temperature can be an important factor for the real application of the biomass. The biosorption of Indigo Carmine and Methylene Blue at a fixed *Mytilus Edulis* shell dose of  $3\text{g.l}^{-1}$  at ambient temperature, 300K and 310K is shown in figure 5. The *Mytilus Edulis* shell showed the maximum biosorption at ambient temperature. An increase in the temperature leads to a decrease in the biosorption capacity at an equilibrium time of 60 minutes, in the order: ambient temperature > 300K > 310K > 320K > 330K.



(a) Indigo Carmine



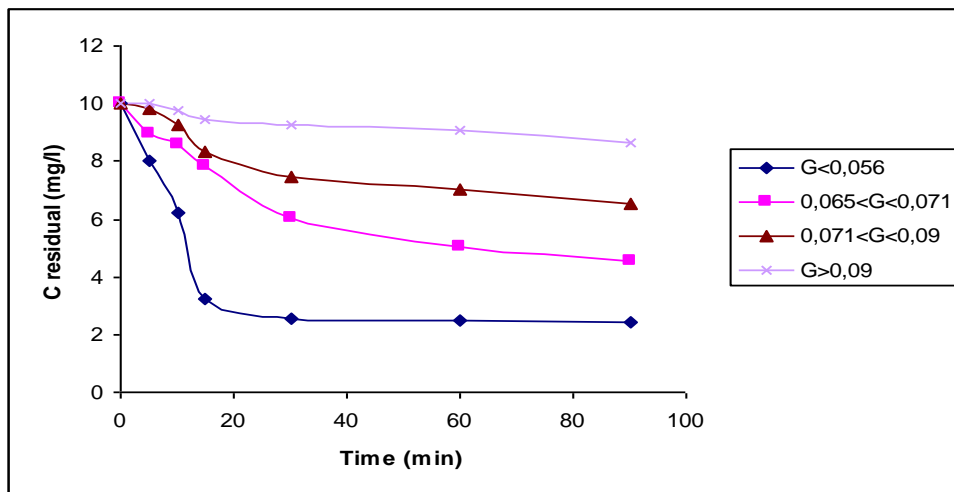
(b) Methylene Blue

**Figure 5:** Variation of dyes biosorption with temperature, pH = 6.8; initial concentration  $40\text{ mg.l}^{-1}$ ; Shell dose  $3\text{ g.l}^{-1}$ ;  $G < 0.056\text{ mm}$

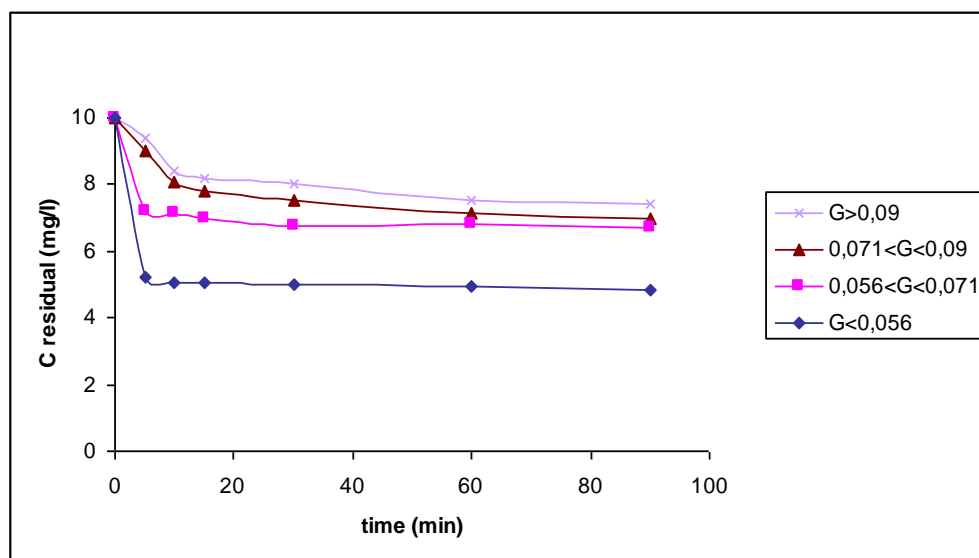
### 3.2.3. Granulometry effect study

The granulometry- effect was studied by comparing four different shell granulometry classes:  $G < 0.056\text{ mm}$ ;  $0.056 < G < 0.071\text{ mm}$ ;  $0.071 < G < 0.09\text{ mm}$ ;  $G > 0.09\text{ mm}$ .

The dyes biosorption equilibrium is quickly reached for the finest granulometry ( $G < 0.056$  mm), while for three other granulometry, the kinetics of elimination is slower (Figure 6). We can conclude that more the shells size is small more the biosorption is better; this is due to the fact that the biosorption depends on the external surface of the biosorbant material which increases with the size smoothness.



(a) Indigo Carmine

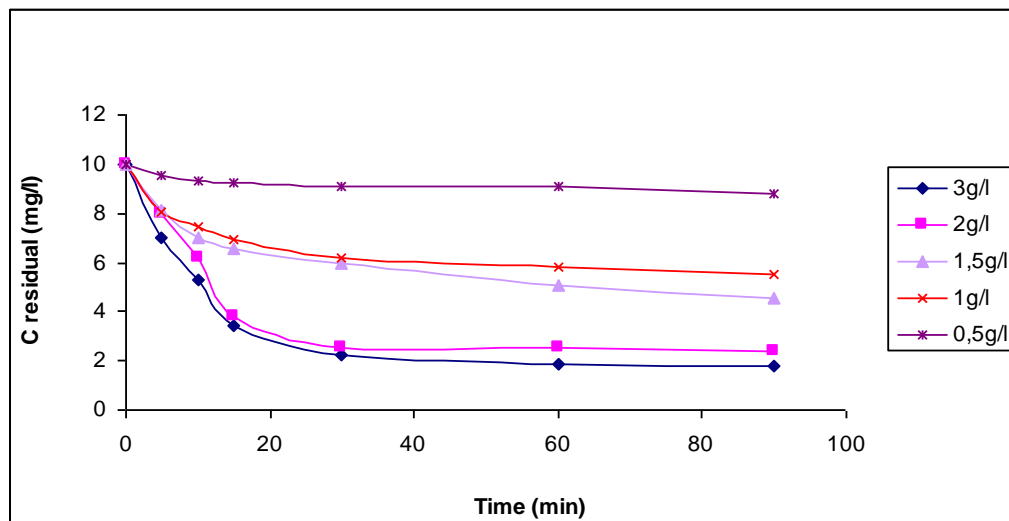


(b) Methylene Blue.

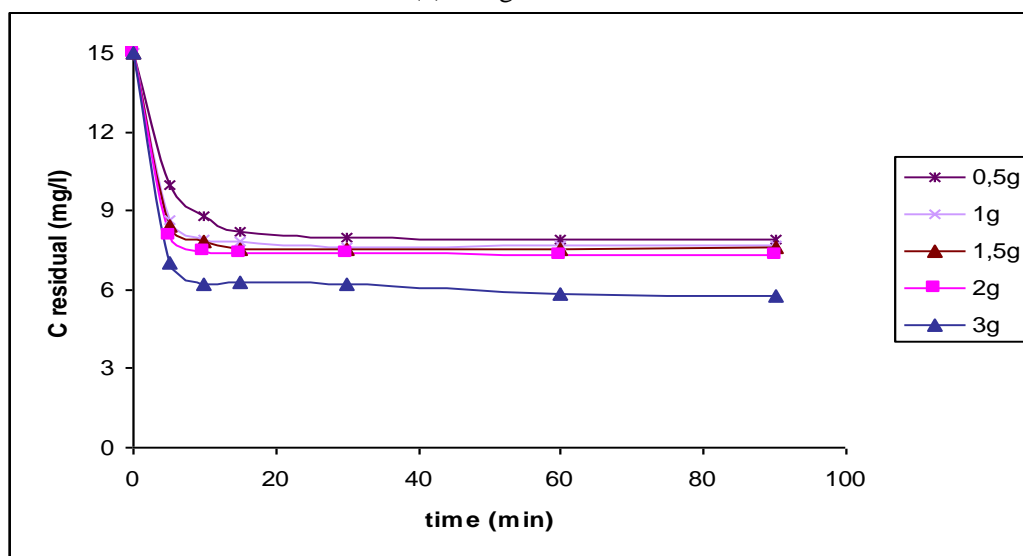
**Figure 6:** Effect of the granulometry on dye biosorption, pH = 6.8; initial concentration  $40 \text{ mg.l}^{-1}$ ; Shell dose  $3 \text{ g.l}^{-1}$ ; Ambient temperature.

#### 3.2.4. Biosorptive doses effect study

The dose effect study, carried out with following dyes residual concentration evolution according to time for different biosorptive doses, is shown in figure 7. The Indigo Carmine and Methylene Blue were practically eliminated from the solution by significant mass of shells  $3 \text{ g.l}^{-1}$  and during a relatively short time (about 60 minutes). The amount of removal degree of dyes increased with the increase in dose of biosorbant. This may be due to the increase in availability of surface active sites resulting from the increased dose and conglomeration of the biosorbents.



(a) Indigo Carmine

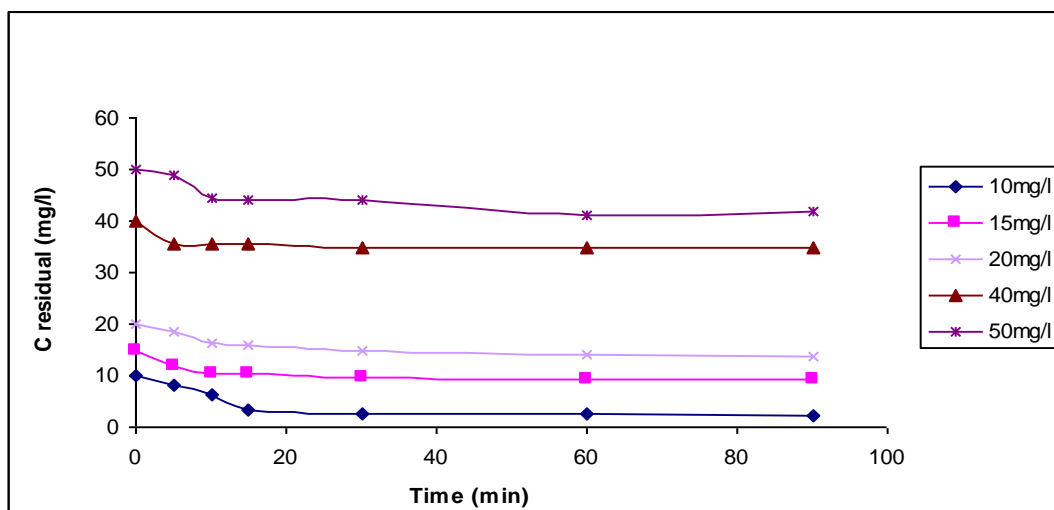


(b) Methylene Blue.

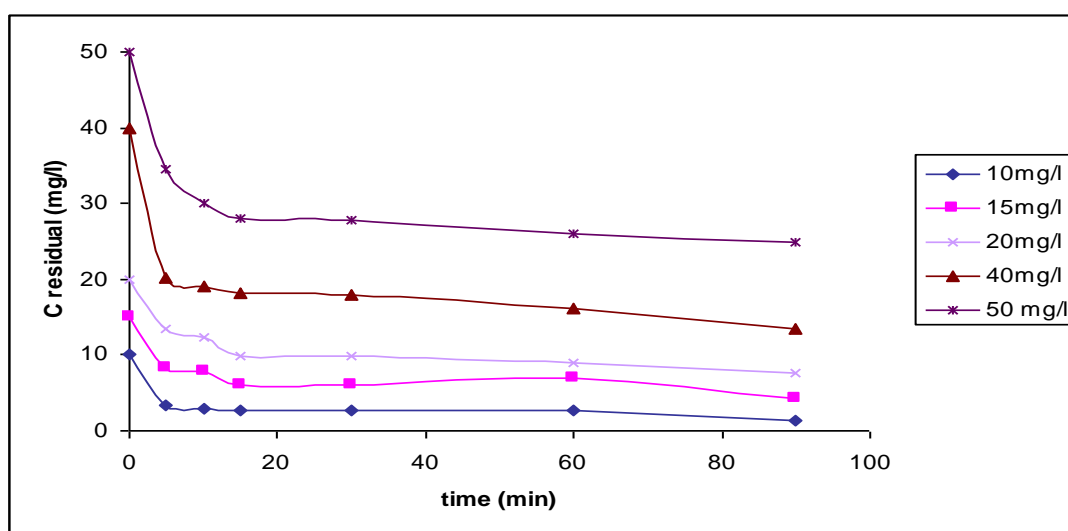
**Figure 7:** Variation of dyes biosorption with biosorptive doses, pH = 6.8; Initial concentration 10 mg.l<sup>-1</sup>; G < 0.056 mm; Ambient temperature.

### 3.2.5. Initial dyes concentration effect study

The dyes concentrations used are selected according to shells mass in order to do not disturb the biosorption phenomenon. The Indigo Carmine and Methylene Blue removal was found to be rapid at the initial period of contact time and then to become slow and stagnate with the increase in contact time until reaching a roughly constant value in about sixty minutes for different concentrations (Figure 8); it shows that the equilibrium time is independent of the initial dye concentration. In addition, we can conclude that the dye concentration should not exceed 10 mg.l<sup>-1</sup> to reach good biosorption.



(a) Indigo Carmine



(b) Methylene Blue

**Figure 8:** Variation of dyes biosorption with initial concentration, pH = 6.8; G < 0.056 mm; Shell dose 2 g.l<sup>-1</sup>; Ambient temperature

### 3.3. Dyes biosorption isotherms

The Freundlich, Langmuir, Elovich and Temkin isotherm models were used to fit the experimental data and these isotherm models are usually adopted for heterogeneous biosorption. Freundlich isotherm relates the adsorbed concentration as the power function of solute concentration. In this isotherm model, the magnitude of  $K_f$  and  $n$  values of the model showed easy uptake of Indigo Carmine from aqueous medium with a high biosorption capacity of the *Mytilus Edulis* shells (Tables 2 and 3). In the case of the Langmuir model, the corresponding plots gave rise to linear plot for the biosorption of Indigo carmine and methylene blue, to *Mytilus Edulis* shell and the correlation coefficient of the plots ( $R^2$ ) was above 0.9 for the concentration 50mg/l, indicating the Langmuir model best fitted the experimental data (Tables 4 and 5).

In the Elovich isotherm, the plot of  $\ln(q_e/C_e)$  according to  $q_e$  achieves the constants  $q_m$  and  $K_E$ . The results are grouped in tables (Table 6 and 7).

The plot of the Temkin isotherm allow us to determine  $B_T$  ( $B_T = q_m RT / \Delta Q$ ), then introducing a value of  $q_m$  (eg after the application of Langmuir) to calculate the variation of adsorption energy  $\Delta Q$  as presented in the following tables (Table 8 and 9).

**Table 2:** The Freundlich models constants and correlation coefficients for biosorption of Carmine indigo on the *Mytilus Edulis* shell

$C_0$ (mg.l <sup>-1</sup> )	$K_f$	$n$	$R^2$	$q_{max}$ (mg.g <sup>-1</sup> )
10	0.539	0.496	0.7895	1.688
	0.534	0.448	0.988	1.498
20	0.227	0.5854	0.7976	1.311
	0.239	0.5803	0.9989	1.359
40	0.484	0.3974	0.8801	2.096
	0.432	0.43	0.9956	2.11
50	0.265	0.322	0.9305	0.933
	0.248	0.395	0.9997	1.162

**Table 3:** The Freundlich models constants and correlation coefficients for biosorption of Methylene blue on the *Mytilus Edulis* shell

$C_0$ (mg.l <sup>-1</sup> )	$K_f$	$n$	$R^2$	$q_{max}$ (mg.g <sup>-1</sup> )
10	1.246	0.434	0.8512	3.384
	1.452	0.478	0.9976	4.364
20	1.258	0.4586	0.8057	4.969
	1.364	0.4474	0.7067	5.21
40	2.474	0.5245	0.844	17.12
	2.38	0.519	0.9959	16.14
50	1.845	0.4867	0.9758	12.38
	1.725	0.488	0.9868	11.63

**Table 4:** The Langmuir models constants and correlation coefficients for biosorption of Carmine indigo on the *Mytilus Edulis* shell

Langmuir forms	$C_0$ (mg.l <sup>-1</sup> )	$K_L$	$q_{max}$	$r^2$	$R_L$
Langmuir I	10	1.468	6.743	0.9158	0.063
Langmuir II		0.047	7.037	0.8672	0.68
Langmuir III		0.048	5.8577	0.9963	0.675
Langmuir IV		0.048	6.2416	0.9963	0.675
Langmuir V		0.048	6.1012	0.9158	0.674
Langmuir I	20	0.138	59.52	0.832	0.266
Langmuir II		0.144	52.08	0.7033	0.257
Langmuir III		0.152	57.908	0.8566	0.247
Langmuir IV		0.13	90.844	0.8566	0.277
Langmuir V		0.15	45.525	0.832	0.249
Langmuir I	40	0.338	21.598	0.8893	0.068
Langmuir II		0.041	20.79	0.7231	0.378
Langmuir III		0.042	15.843	0.9987	0.373
Langmuir IV		0.042	16.235	0.9987	0.373
Langmuir V		0.042	16.411	0.7893	0.371
Langmuir I	50	0.143	25.974	0.8206	0.127
Langmuir II		0.028	48.31	0.6355	0.432
Langmuir III		0.028	33.553	0.9693	0.412
Langmuir IV		0.276	40.41	0.9693	0.42
Langmuir V		0.028	31.211	0.7634	0.409

**Table 5:** The Langmuir models constants and correlation coefficients for biosorption of methylene blue on the *Mytilus Edulis* shell

Langmuir forms	$C_0$ (mg.l <sup>-1</sup> )	$K_L$	$q_{max}$	$r^2$	$R_L$
Langmuir I	10	0.99	14.2	0.8643	0.092
Langmuir II		0.026	14.47	0.829	0.793
Langmuir III		0.0265	10.403	0.9985	0.79
Langmuir IV		0.0265	10.76	0.9985	0.79
Langmuir V		0.0263	12.125	0.8643	0.792
Langmuir I	20	0.149	95.23	0.8271	0.251
Langmuir II		0.162	77.52	0.643	0.235
Langmuir III		0.183	53.564	0.9856	0.214
Langmuir IV		0.1806	56.73	0.9856	0.217
Langmuir V		0.1697	69.23	0.8271	0.227
Langmuir I	40	0.91	5.66	0.8316	0.027
Langmuir II		0.025	5.437	0.458	0.5
Langmuir III		0.026	3.1689	0.9978	0.49
Langmuir IV		0.0262	3.263	0.5316	0.488
Langmuir V		0.265	2.788	0.5316	0.485
Langmuir I	50	0.81	3.43	0.9083	0.024
Langmuir II		0.022	3.441	0.8969	0.476
Langmuir III		0.022	3.4812	0.9996	0.476
Langmuir IV		0.0218	3.509	0.9996	0.478
Langmuir V		0.022	3.091	0.9083	0.476

**Table 6:** The Elovich model constants and correlation coefficients for biosorption of Indigo Carmine on the *Mytilus Edulis* shell

$C_0$ (mg.l <sup>-1</sup> )	$q_m$	$\ln(K_E \cdot q_m)$	$r^2$	$K_E$
10	250	0.8157	0.9516	0.009
20	222	0.68	0.9593	0.0089
40	43.29	-0.8785	0.9792	0.009
50	63.29	-0.5281	0.9746	0.009

**Table 7:** The Elovich model constants and correlation coefficients for biosorption of Methylene Blue on the *Mytilus Edulis* shell

$C_0$ (mg.l <sup>-1</sup> )	$q_m$	$\ln(K_E \cdot q_m)$	$r^2$	$K_E$
10	86.95	0.2221	0.9353	0.014
20	243.9	2.7491	0.7705	0.015
40	188.6	1.0261	0.9964	0.014
50	212.76	0.8616	0.9556	0.011

**Table 8:** The Temkin model constants and correlation coefficients for biosorption of Indigo Carmine on the *Mytilus Edulis* shell

$C_0$ (mg.l <sup>-1</sup> )	$B_T$	$r^2$	$K_T$	$\Delta Q$	$q_m$
5	840.82	0.988	0.058	25.3	8.583
10	2627.6	0.648	0.031	13.65	14.47
20	125.54	0.458	1.033	15.3	77.52
40	323.26	0.604	0.032	41.69	5.437
50	955.26	0.921	0.024	8.929	3.441

**Table 9:** The Temkin model constants and correlation coefficients for biosorption of Methylene Blue on the *Mytilus Edulis* shell

$C_0$ (mg.l <sup>-1</sup> )	$B_T$	$r^2$	$K_T$	$\Delta Q$	$q_m$
5	114.98	0.825	0.403	2422.1	112.35
10	542.85	0.689	0.064	32.13	7.037
20	172.14	0.498	0.99	749.95	52.79
40	1201.3	0.667	0.055	42.89	20.79
50	771.05	0.823	0.044	155.31	48.31

### 3.4. Biosorption equilibrium time and kinetic models

Biosorption rates of dyes were obtained by recording the gradual decrease of the concentration of dye within the adsorption medium with time. The time necessary to reach equilibrium for the removal of the Indigo Carmine and Methylene Blue by *Mytilus Edulis* shells from aqueous solution was established about 1h. After equilibrium, the amount of biosorbed dyes did not change significantly with time. The experimental kinetic data of biosorption studies were applied to the pseudo first and pseudo second order kinetic models. First-order kinetic indicates that the process of biosorption occurs at a rate proportional to dye concentration, which is particularly suitable for low concentrations. Pseudo second order kinetic is thought to drive from biosorption processes in which the rate-controlling step is an exchange reaction. The rate constants, K, for the biosorption of the Indigo Carmine and Methylene Blue on *Mytilus Edulis* shells were determined from the pseudo first and pseudo second order rate equation. The data obtained by the pseudo first order kinetic equation describe well the reactions and the mechanisms of Indigo Carmine and Methylene Blue biosorption on *Mytilus Edulis* shells because the rate coefficients  $K_1$  is a constant for the pseudo first order kinetic models (Table 10 and 11).

**Table 10:** The first and second order kinetic constants for Indigo Carmine biosorption on *Mytilus Edulis* shells

$C_0$ (mg.l <sup>-1</sup> )	Pseudo first order kinetic			Pseudo second order kinetic		
	$r^2$	$q_e$	$K_{1\text{ app}}$	$r^2$	$q_e$	$K_{2\text{ app}}$
10	0.9101	7.831	0.039	0.995	7.8318	0.037
20	0.9754	6.374	0.037	0.9994	6.374	0.384
40	0.8978	6.6	0.037	0.9926	6.6	0.976
50	0.9331	10	0.031	0.9996	10	0.752

**Table 11:** The first and second order kinetic constants for Methylene Blue biosorption on Mytilus Edulis shells

$C_0$ (mg.l <sup>-1</sup> )	Pseudo first order kinetic			Pseudo second order kinetic		
	r <sup>2</sup>	q <sub>e</sub>	K <sub>1 app</sub>	r <sup>2</sup>	q <sub>e</sub>	K <sub>2 app</sub>
10	0.9401	8.632	0.018	0.9988	8.632	0.206
20	0.9	12.334	0.025	0.9946	12.334	0.024
40	0.9174	26.438	0.024	0.9929	26.438	0.012
50	0.9359	25	0.02	0.9993	25	0.044

3.5. Comparison of Mytilus Edulis biosorption capacities with marine algae, wood sawdust and actived carbon

Batch biosorption of Indigo Carmine, up to 10 mg.l<sup>-1</sup>, onto Mytilus Edulis shells was studied in comparison with Marine Algae, wood sawdust and Actived carbon, in order to explore the potential use of this material as low cost adsorbent for dye removal in textile effluents. According to this comparative study, we can consider the activated carbon as the best biosorbents (Figure 9). But if we take account of the biosorbents cost and the contaminant that is sometimes difficult to eliminate, the shells Mytilus Edulis could be employed as alternatives to commercial activated carbon in wastewater treatment.

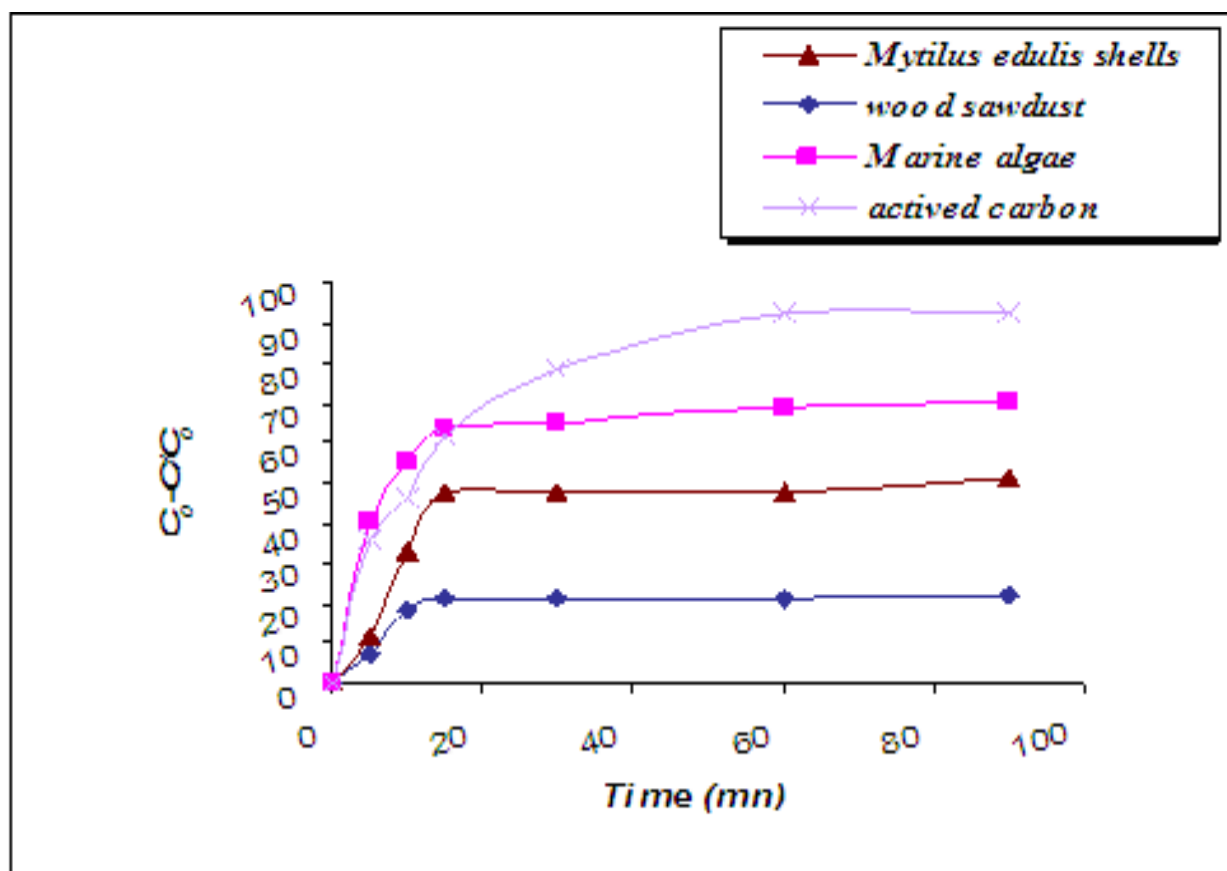


**Figure.9:** Comparison of Mytilus Edulis biosorption capacities with actived charbon, marine algae and Wood sawdust

## Conclusion

This study highlighted the capacities of *Mytilus Edulis* shells to pre-treat dyeing raw wastewaters. The extent of dye removal increased with decrease in the initial concentration of the dye and particle size of the biosorbents and also increased with increase in contact time and the amount of biosorbents used. The equilibrium biosorption is practically achieved in 60 min. Biosorption data were modelled using the Freundlich, Langmuir, Elovich and Temkin adsorption isotherms and the kinetic was investigated by the pseudo first and pseudo second order kinetic equations. The biosorption capacities of *Mytilus Edulis* shells have been compared with that of the marine algae, wood sawdust and activated carbon. The results indicate that *Mytilus Edulis* shells could be employed as low cost alternative to commercial activated carbon in wastewater treatment for the methylene blue and Indigo Carmine removal.

To sum up, the Shells “*Mytilus Edulis*” presents a potential to be used as a biosorbents material for the methylene blue and indigo carmine removal from aqueous solutions because of abundance, its low cost, high biosorption capacity and reasonable rapid rate of biosorption as well as being free from pathogenicity.

## References

1. R. Seed. «Ecology. In Marine mussels; their ecology and physiology». Ed. Bayne BL. Cambridge University Press, Cambridge. (1976).
2. P. Hovgaard, S. Mortensen, Ø, Strand. Skjell – «biologi og dyrking». Kystnæringen Forlag & bokklubb AS, ED 1, (2001).
3. H. Zollinger, «Color chemistry syntheses, properties and applications of organic dyes and pigments»VCH publications, Weinheim, Allemagne, (1991)
4. P. Cooper, « Colour in dyehouse effluent »,the society of dyers and colourists, Nottingham, (1995)
5. A. Anliker, « Ecotoxixology off dyestuffs – a joint effort by industry Ecotoxicol», environ. Safety (1979).
6. A. Mittal, J. Mittal, L. Kurup, «Batch and bulk removal of hazardous dye, indigo Carmine from wastewater through adsorption», Department of Applied Chemistry, National Institute of Technology, India, (2006).
7. Y. S.Sheykin, C.Starr, P.S. Li,M. Goldstein «Effect of Methylene Blue, Indigo Carmine and Renografin on Human Sperm », Center for male Reproduction and Microsurgery, Departement of Urology, New York , Hospital Cornell Medical Center and the population Concil, Center for Biomedical Research, New York.
8. H. Freundlich, Kapillarchemie. Akademische Verlagsgesellschaft, Leipzig, Synthesis and catalysis, 4 (1909).
9. I. Langmuir, the adsorption of gases on plane surfaces of glass, mica and platinum, Journal of American Chemical Society, 40 (1918) 1361.
10. O. Hamdaoui, E. Naffrechoux, Modeling of adsorption isotherms of phenol and chlorophenols onto granular activated carbon. Part I. Two-parameter models and equations allowing determination of thermodynamic parameters, Hazardouz Materials, (1909).
11. S.Y. Elovich, O.G. Larinov, “Theory of adsorption from solutions of non electrolytes on solid (I) equation adsorption from solutions and the analysis of its simplest form (II), verification of the equation of adsorption isotherm from solutions”, Izv. Akad. Nauk. SSSR, Otd.Khim. Nauk, (1962).
12. M.J. Temkin, V. Pyzhev, Kinetics of ammonia synthesis on promoted iron catalysts, Acta Physicochim, URSS, (1940),.
13. J. Toth, State equations of the solid gas interface layer, Acta Chemistry Academia Science, Hungaria, (1971),.
14. C. Hinz, Description of sorption data with isotherm equations, Geoderma, (2001).
15. G. Limousin, J.P. Gaudet, L. Charlet, S. Szenknect, V. Barthes, M. Krimissa Sorption isotherms: A review on physical bases, modelling and measurement –Applied Geochemistry, (2007).
16. O. Hamdaoui, Batch study of liquid-phase adsorption of methylene blue using cedar sawdust and cruched brick, Hazardous Materials, (2006).

17. B.H. Hameed, Equilibrium and kinetic studies of methyl violet sorption by agricultural waste, *ournal of Harzardous Materials*, (2007).
18. F. Gimbert, N.M. Crini, F. Renault, P.M. Badot, G. CrinI, Adsorption isotherm models for dye removal by cationized starch-based material in a single component system: Error analysis, *Journal of Hazardous Materials*. (2008),
19. S. Lagergen, *K Sven Vetenskapsakad Handl*, (1898).
20. M. Sarkar, P.M. Acharya, B. Bhattacharya, Modeling the adsorption kinetics of some priority organic pollutants in water from diffusion and actived energy parameters *Journal of colloid and interface Science*, (2003).
21. Y. S. Ho, G. Mckay, A Two- StageBatch sorption optimized Design for dye removal to minimize contact time, *Process safety Environnement Protection*, (1998).
22. Y. S. Ho, G. Mckay, The kinetics of sorption of divalent metal ions onto sphagnum moss peat, *Water Research*, (2000).
23. Silverstein Bassler, Morill, And Jean Umber «Spectrometric idendification of organic compounds» *Lycée Louis Vincent à Metz*.
24. H. Aderdour, A. Bentayeb, A. Dekayir, A. Yacoubi and A. Nadiri, «Investigation on two Moroccan Diatomites, 8 Th Moroccan Metting on Solid State Chemistry», *Univerité Abdelmalek Essaadi, Faculty of Sciences.Morroco, Tetouan 27-29 octobre.(1999)*,
25. R Bouchta. and A. Mareil, «In Morrocan oil shale Development Program», 6 th. *NASA Ressources Conférence, Golden, Colorad, USA, (1981)*.
26. H. Vanolphen, J. Fripiat, in «Data Handbook for clay Materials and other Non metallic Minerals» *Peganon Press, London, (1979)*.
27. G. Socrates, «Infrared characteristic Group Frequencies», (1980), p: 126.

(2012) [www.jmaterenvironsci.com/](http://www.jmaterenvironsci.com/)